gene ontology, pathway, and WGCNA module enrichment. The Wilcoxon rank sum test was used to calculate cluster markers within Seurat[23]. Three independent snRNA-seq experiments were performed. Gene set enrichment analysis was performed using a one-sided Z-test and *P* values were adjusted using the Bonferroni method.

Extended Data

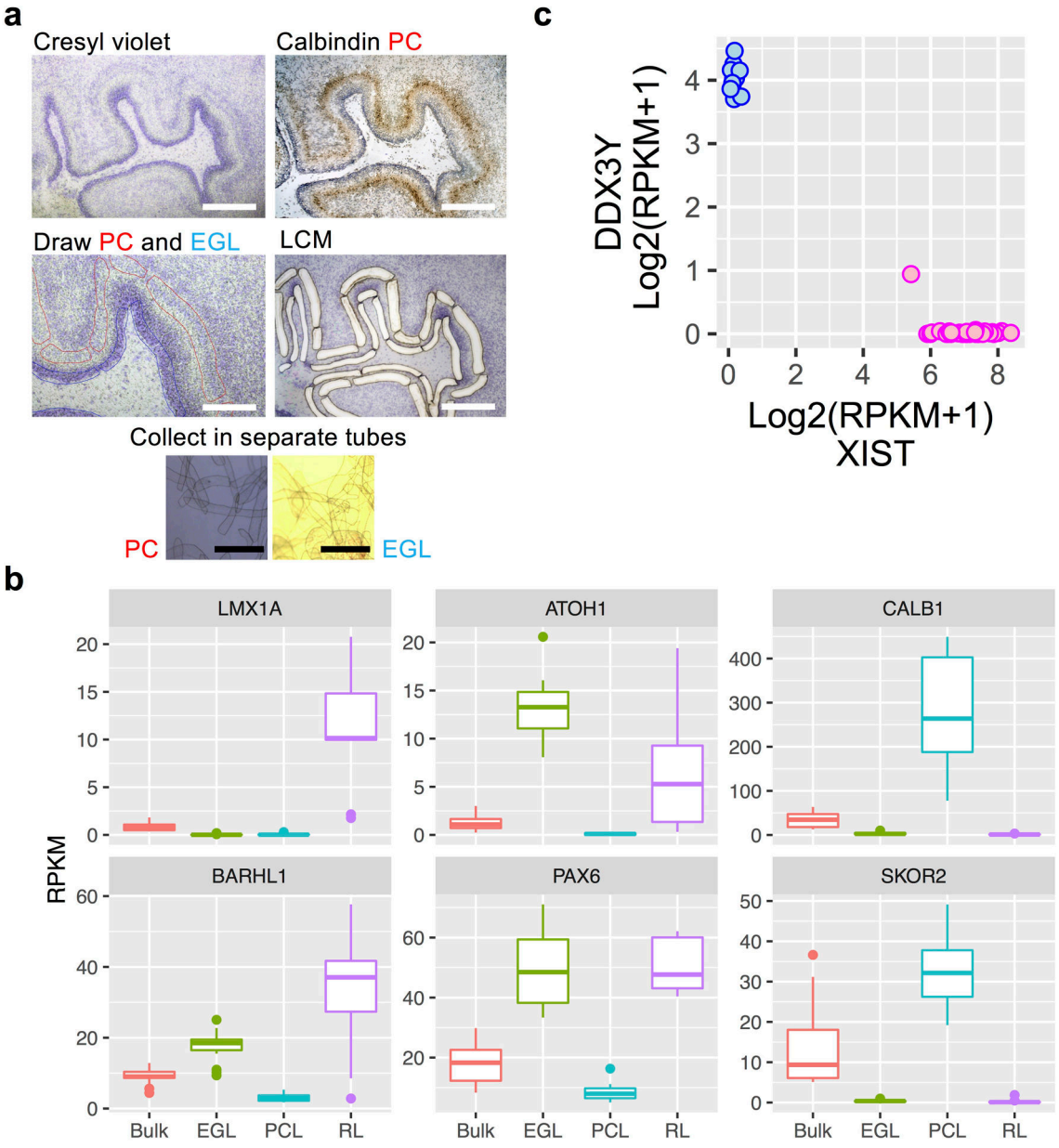

Extended Data Fig. 1. Quality control related analyses of LCM RNA-seq data.

a, Example of cerebellum section stained with cresyl violet (purple) and anti-calbindin antibody (brown). Section before and after LCM and images of Purkinje cell (PC) and external granule cell layer (EGL) tissue captured into collection tubes are shown. Example shown is representative of 11 specimens. Scale bars: 200 um (white), 400 um (black). **b,**

Boxplots of gene expression for established markers showing highest expression in the expected samples (box: 25–75th percentiles, whiskers: 10–90th percentiles, horizontal line in box: median). Dots indicate outliers. RNA-seq sample numbers per region: n = 13 for bulk; 17 for EGL; 18 for PCL; 9 for RL. **c,** Expression of the female-specific non-coding RNA *XIST* and the chromosome Y specific gene *DDX3Y* show correct sex assignment for female (pink) and male (blue) samples. RNA-seq sample numbers: n = 13 for bulk; 17 for EGL; 18 for PCL; 9 for RL. RNA-seq sample numbers per sex: n = 44 female; 13 male.

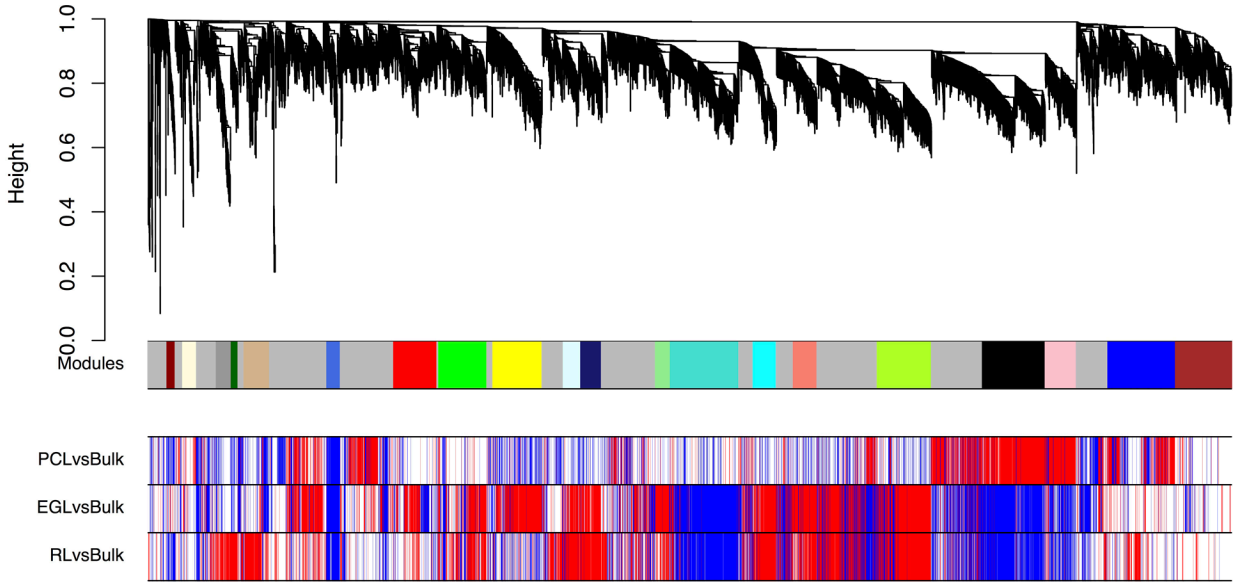

Extended Data Fig. 2. Co-expression modules in the developing human cerebellum.
Weighted gene co-expression network analysis (WGCNA) dendrogram identified 21 modules comprised of 6,336 expressed genes (row 1). M0 (grey) comprised of nonclustered genes was not analyzed further. Rows 2–4 show differential expression relationships between module genes and LCM-enriched region compared to bulk expression. EGL, external granule cell layer; PCL, Purkinje cell layer; RL, rhombic lip.

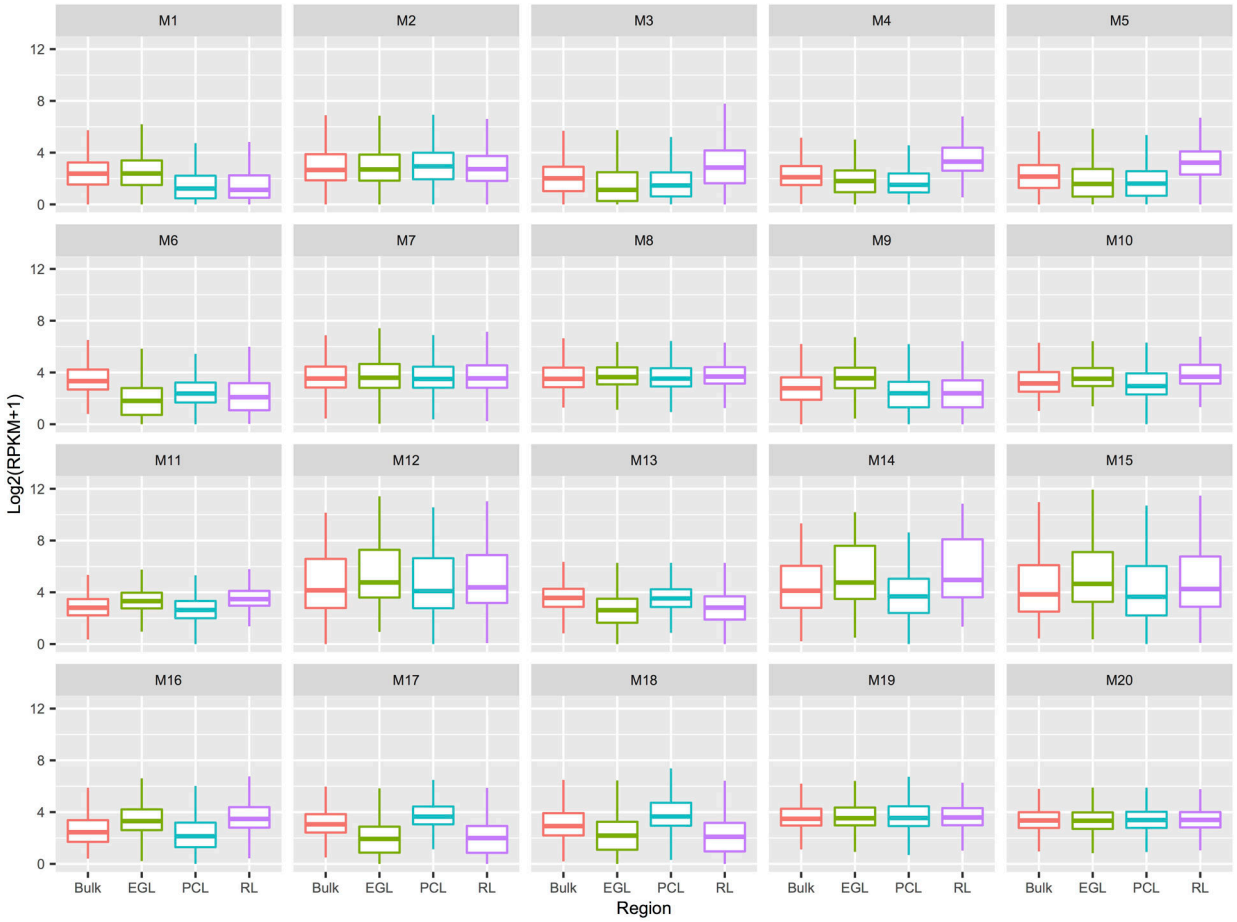

Extended Data Fig. 3. Co-expression modules in the developing human cerebellum by region.

Boxplots of gene expression per WGCNA module for bulk and spatial regions (box: 25–75th percentiles, whiskers: 10–90th percentiles, horizontal line in box: median). Number of genes per module: n = 48 for M1; 81 for M2; 88 for M3; 40 for M4; 149 for M5; 79 for M6; 253 for M7; 283 for M8; 288 for M9; 102 for M10; 121 for M11; 87 for M12; 401 for M13; 136 for M14; 139 for M15; 317 for M16; 367 for M17; 182 for M18; 395 for M19; 327 for M20. EGL, external granule cell layer; PCL, Purkinje cell layer; RPKM, reads per kilobase of transcript per million mapped reads; RL, rhombic lip.

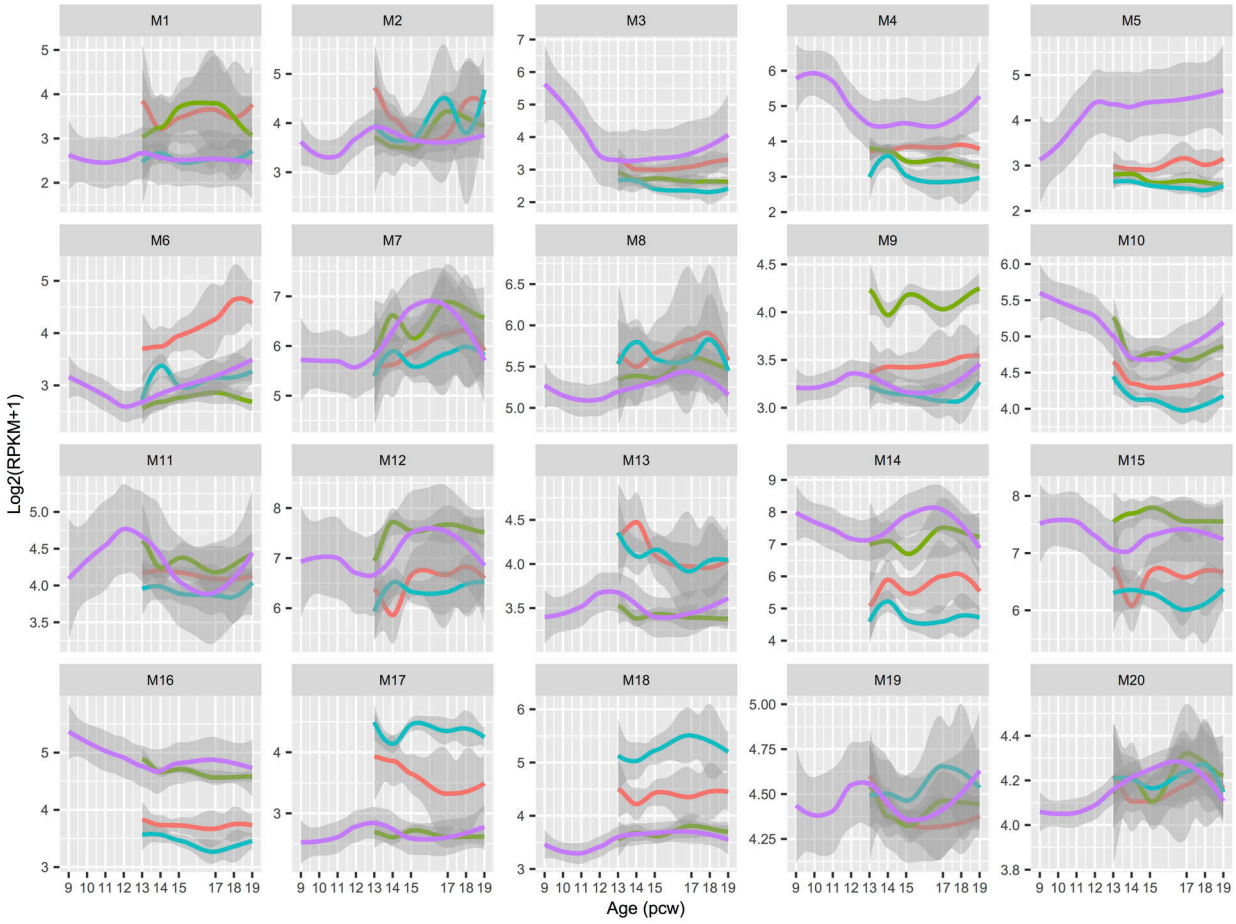

Extended Data Fig. 4. Co-expression modules in the developing human cerebellum by age.
LOESS expression values across development are shown with 95% CIs per module. Spatial regions are distinguished by colors: bulk (salmon); EGL (green); PCL (turquoise); RL (purple). EGL, external granule cell layer; PCW, postconceptional week; PCL, Purkinje cell layer; RPKM, reads per kilobase of transcript per million mapped reads; RL, rhombic lip.

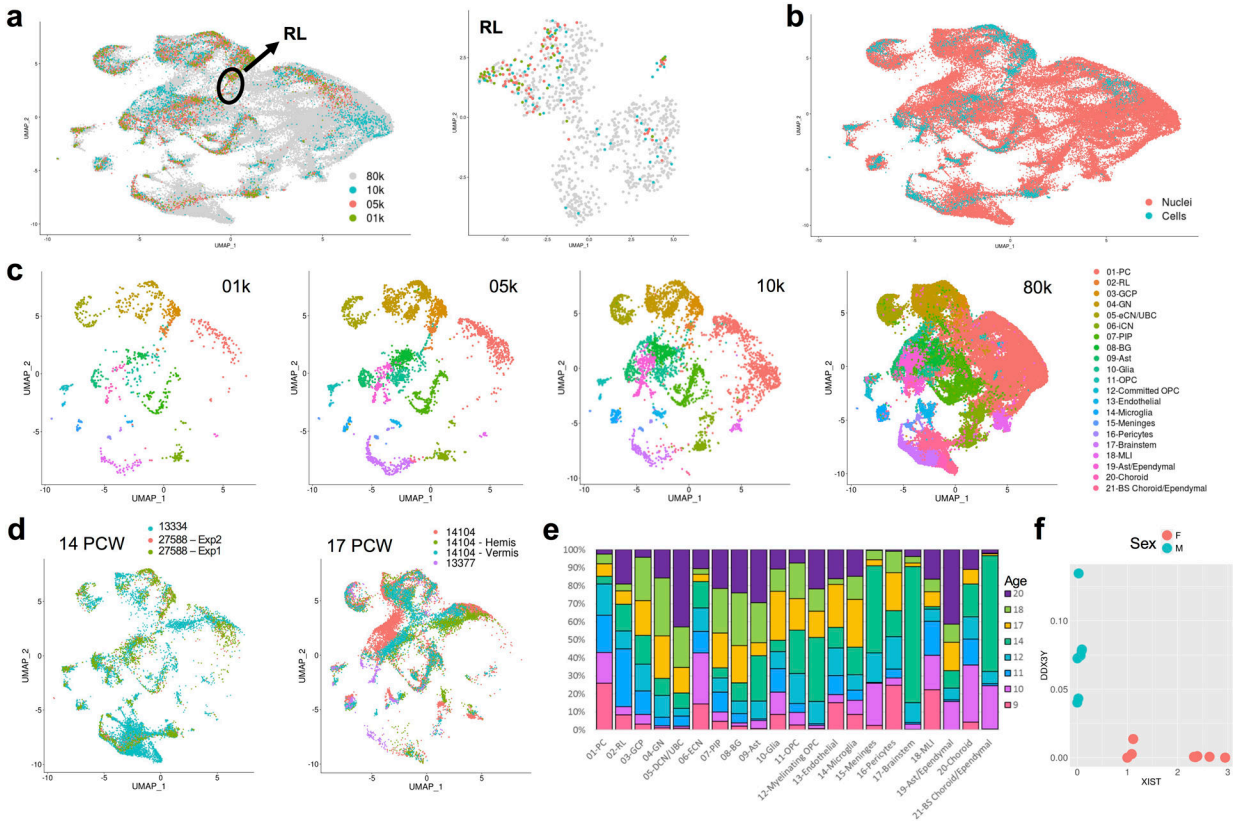

Extended Data Fig. 5. Quality control related analyses of snRNA-seq data.

a, UMAP visualization of 69,174 human cerebellar nuclei colored by dataset (n = 1,076 for 01k; 3,530 for 05k; 4,960 for 10k; 59,608 for 80k). Rhombic lip (RL) is circled. UMAP visualization of 1,018 RL nuclei colored by dataset at right (nuclei numbers: n = 41 for 01k; 88 for 05k; 67 for 10k; 822 for 80k). **b,** The same UMAP as in **a** with nuclei colored by type (n = 4,462 cells; 64,712 nuclei). **c,** The same UMAP as in **a** and **b** showing nuclei from each dataset. Nuclei are colored by cell type. **d,** The same UMAP as in **a-c** showing nuclei sampled from same age biological and technical replicates (n = 11,213 for 14 PCW; 8,453 nuclei for 13334; 2,098 cells for 27588 Exp1; 662 cells for 27588 Exp2; n = 15,556 for 17 PCW; 524 cells for 13377; 8,540 nuclei for 14104; 3,364 nuclei for 14104h; 3,128 nuclei for 14104v). **e,** Stacked bar chart shows the percentage of age sampled in each of the 21 cell types. Bar colors represent age sampled in postconceptional weeks (9–20 PCW). **f,** Expression of the female-specific non-coding RNA *XIST* and the chromosome Y specific gene *DDX3Y* show correct sex assignment for female (salmon) and male (turquoise) samples (n = 14 female; 12 male).

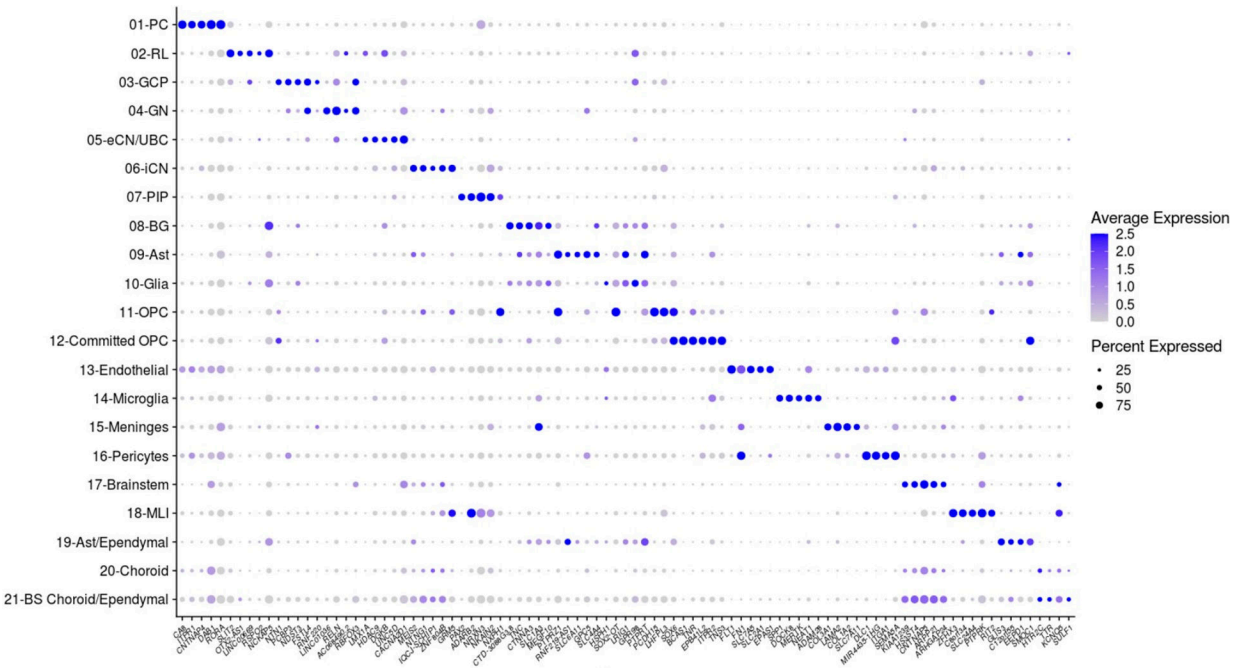

Extended Data Fig. 6. Cell-type-specific marker genes.

Dot plot showing expression of the top 5 most differentially expressed genes for each of the 21 cell types identified in early and mid-gestation fetal cerebellum. The size of the dot represents the percentage of cells within a cell type in which that gene was detected and its color represents the average expression level. Statistics are presented in Supplementary Table 9.

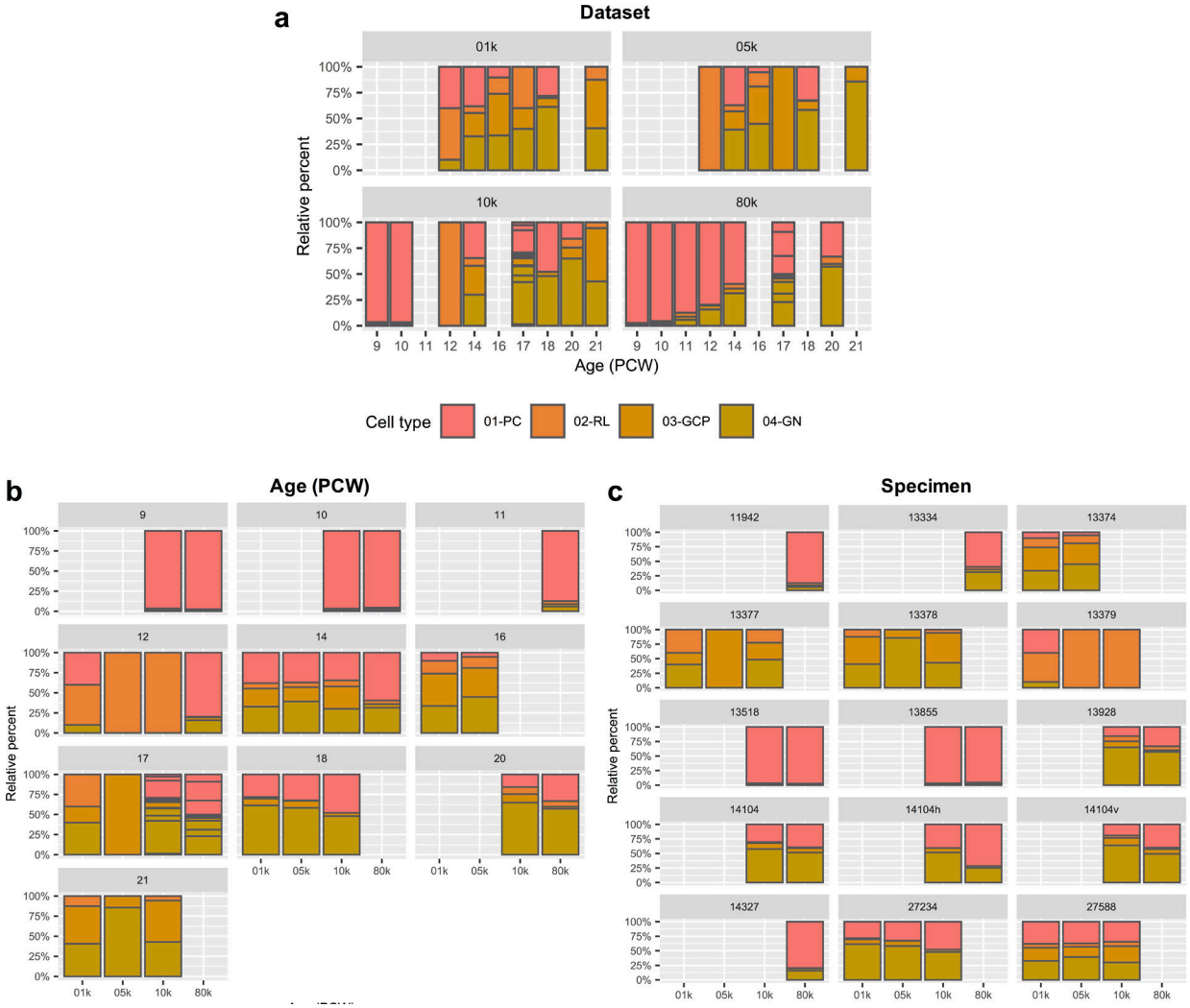

Extended Data Fig. 7. Distribution of major cell types.

a-c, Stacked bar charts show the percentage of the four major cell types from each dataset (a), developmental age (b), and specimen (c). Dataset 01k and 05k from experiment (Exp) 1 represent deep and shallow sequencing runs, respectively, from the same 6 samples (one per age). Dataset 10k from Exp 2 represents 11 samples (7 for a single age and 4 for 17 PCW), including 5 replicates from Exp 1. Dataset 80k from Exp 3 represents 9 samples (6 for a single age and 3 for 17 PCW), including 6 replicates from Exp 2. Sample and experiment characteristics are presented in Supplementary Table 2 and 7.

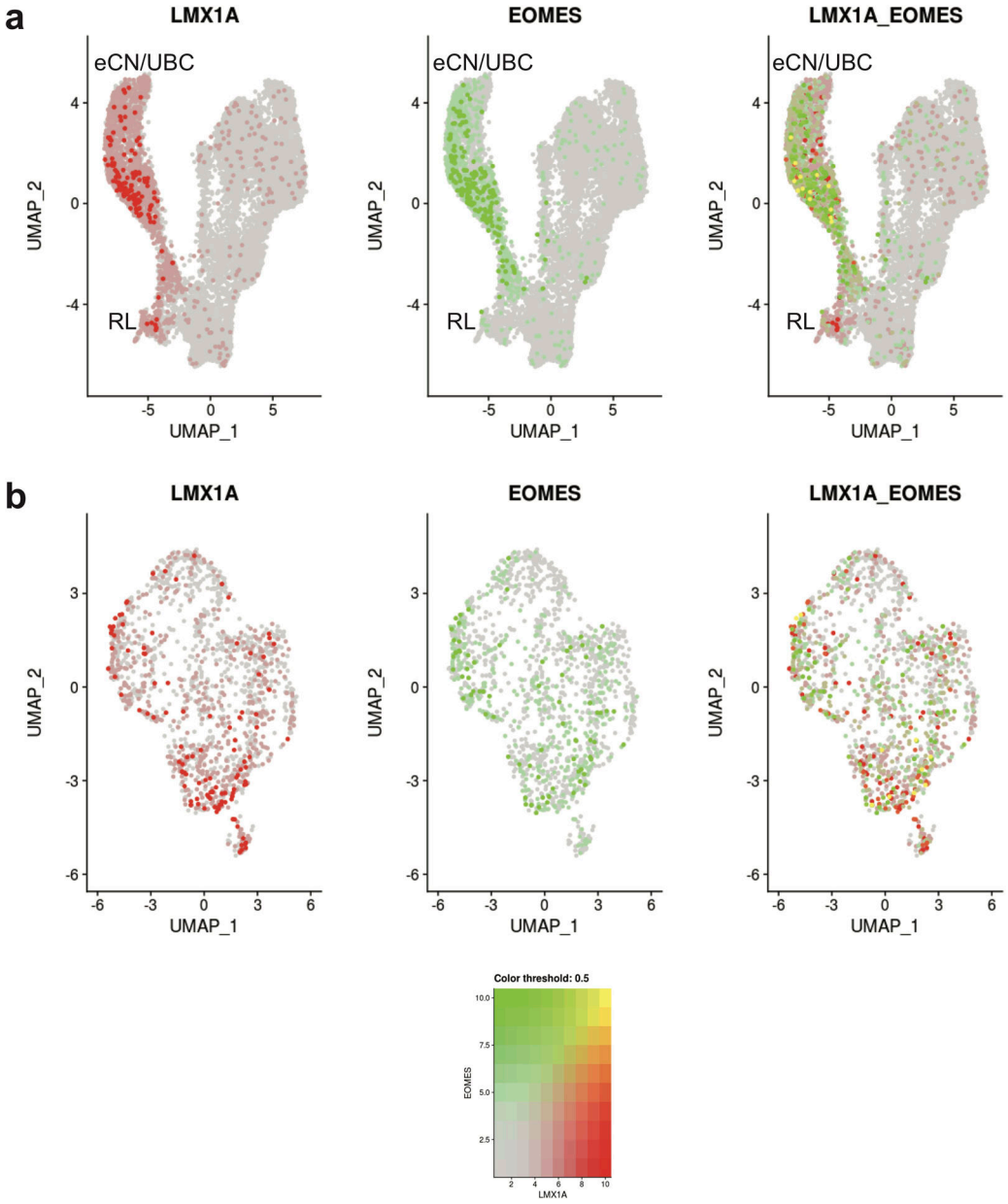

Extended Data Fig. 8. Co-expression of marker genes in eCN/UBC.

a, The same UMAP visualization of cell types that originate from the RL as in Fig. 5a with nuclei colored by expression level for *LMX1A* (red), *EOMES* (green), and co-expression (yellow). **b,** The same UMAP visualization the eCN/UBC subcluster as in Fig. 5e with nuclei colored by expression level for *LMX1A* (red), *EOMES* (green), and co-expression (yellow).

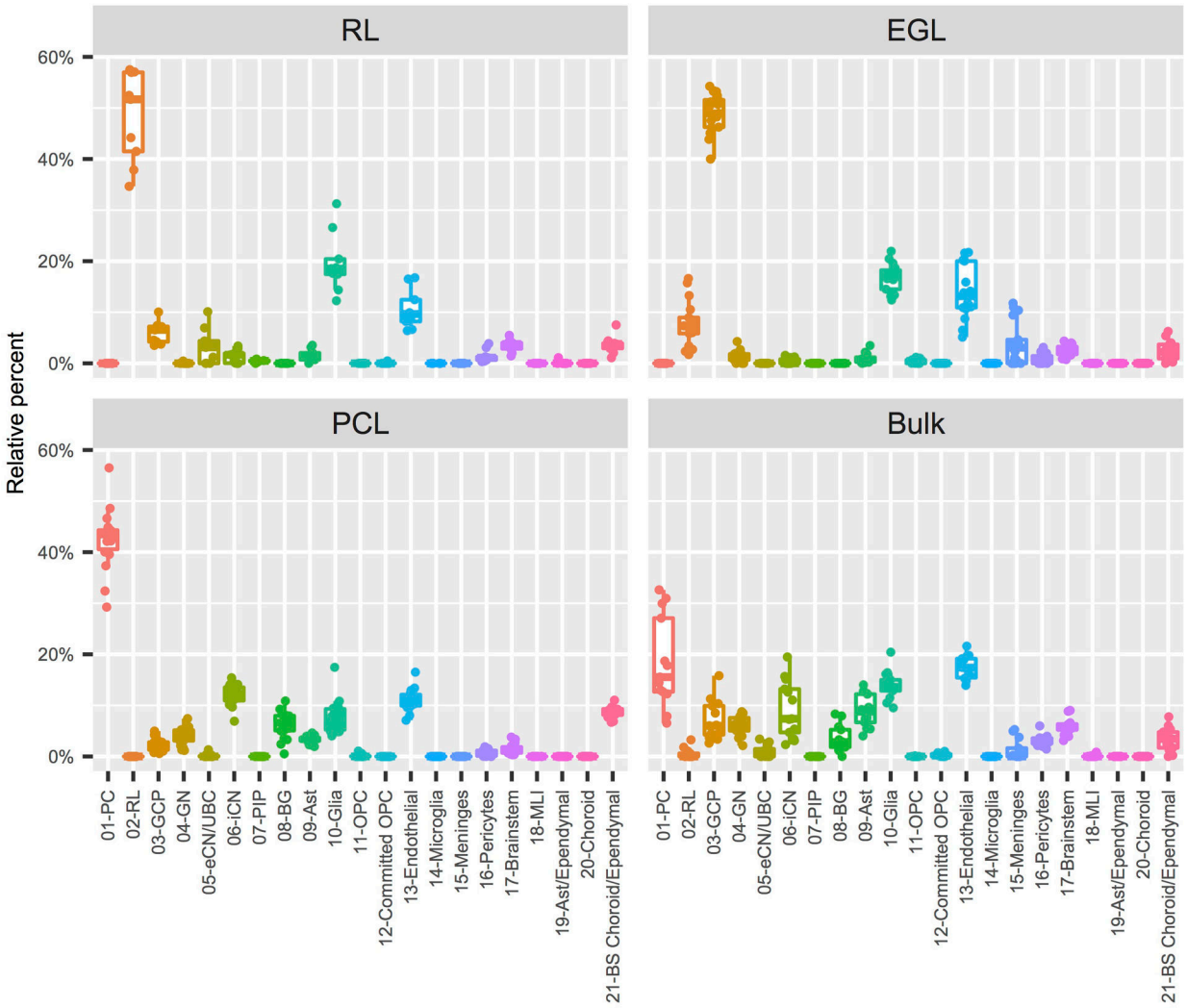

Extended Data Fig. 9. Cell type heterogeneity in LCM-isolated regions of the cerebellum.

Box plots (box: 25–75th percentiles, whiskers: 10–90th percentiles, horizontal line in box: median) with data points (dots) showing the proportion of each of the 21 cell types from the *Developmental Cell Atlas of the Human Cerebellum* represented in the LCM RNA-seq data, grouped by LCM-isolated region. RL, rhombic lip; EGL, external granule cell layer; PCL, Purkinje cell layer.

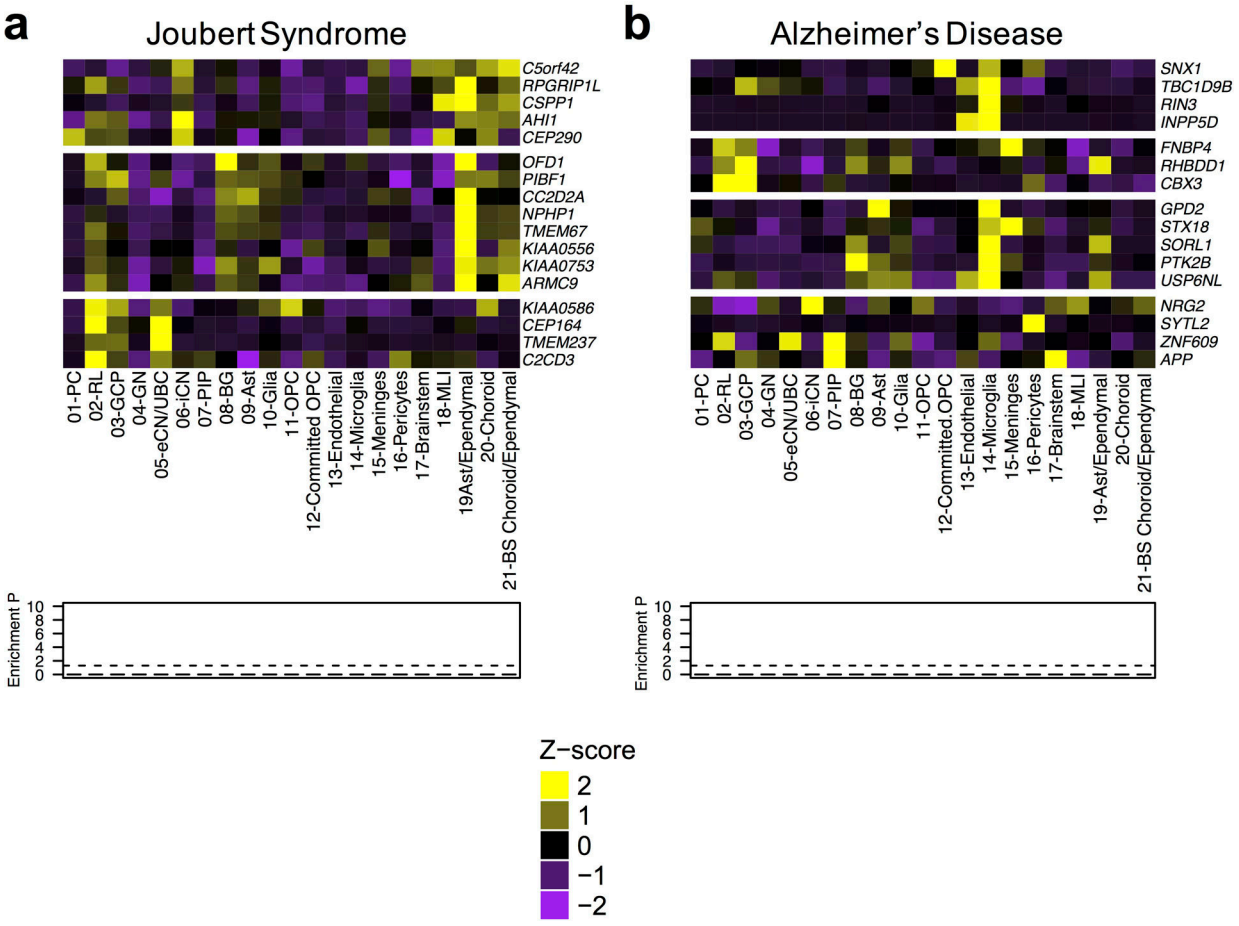

Extended Data Fig. 10. Cerebellar cell type enrichment in Joubert syndrome and Alzheimer's disease.

Heatmaps of mean expression per fetal cerebellar cell type for genes associated with Joubert syndrome (**a**) or Alzheimer's disease (**b**). Color scheme is based on Z-score distribution. In the heatmaps, each row represents one gene and each column represents a single cell type. Horizontal white lines indicate branch divisions in the clustering dendrograms (not shown). The full list of genes is provided in Supplementary Table 11. Enrichment *P* values (-Log10 P value) for each cell type are shown in the bottom bar plots. Significance determined by one-sample Z-test, two-tailed *P* value. The dashed line is the Bonferroni significance threshold ($P<0.05$); no gene enrichment was detected among the 21 cerebellar cell types.

Supplementary Material

Refer to Web version on PubMed Central for supplementary material.

Acknowledgements

This study was funded by the National Institutes of Health under National Institute of Neurological Disorders and Stroke (NINDS), National Institute of Child Health and Human Development (NICHD), and National Institute of Mental Health (NIMH) grant numbers NS095733 to K.J.M., HD000836 to I.A.G., NS050375 to W.B.D, and MH110926, MH116488, and MH106934 to N.S. The project that gave rise to these results received the support of a fellowship from "la Caixa" Foundation (ID 100010434) to G. Santpere. The fellowship code is LCF/BQ/PI19/11690010. K.A.A. received a Parental Leave Grant from Life Science Editors and would like to thank Dr.

Christina Lilliehook for editorial assistance. This publication is part of the Human Cell Atlas - www.humancellatlas.org/publications

REFERENCES

1. Sathyanesan A, et al. Emerging connections between cerebellar development, behaviour and complex brain disorders. Nat Rev Neurosci 20, 298–313 (2019). [PubMed: 30923348]
2. Schmahmann JD The cerebellum and cognition. Neurosci Lett 688, 62–75 (2019). [PubMed: 29997061]
3. Leto K, et al. Consensus Paper: Cerebellar Development. Cerebellum 15, 789–828 (2016). [PubMed: 26439486]
4. Rakic P & Sidman RL Histogenesis of cortical layers in human cerebellum, particularly the lamina dissecans. J Comp Neurol 139, 473–500 (1970). [PubMed: 4195699]
5. Aldinger KA & Doherty D The genetics of cerebellar malformations. Semin Fetal Neonatal Med 21, 321–332 (2016). [PubMed: 27160001]
6. Hoxha E, et al. The Emerging Role of Altered Cerebellar Synaptic Processing in Alzheimer's Disease. Front Aging Neurosci 10, 396 (2018). [PubMed: 30542279]
7. Klockgether T, Mariotti C & Paulson HL Spinocerebellar ataxia. Nat Rev Dis Primers 5, 24 (2019). [PubMed: 30975995]
8. Corrales JD, Rocco GL, Blaess S, Guo Q & Joyner AL Spatial pattern of sonic hedgehog signaling through Gli genes during cerebellum development. Development 131, 5581–5590 (2004). [PubMed: 15496441]
9. Dahmane N & Ruiz i Altaba A Sonic hedgehog regulates the growth and patterning of the cerebellum. Development 126, 3089–3100 (1999). [PubMed: 10375501]
10. Haldipur P, et al. Spatiotemporal expansion of primary progenitor zones in the developing human cerebellum. Science 366, 454–460 (2019). [PubMed: 31624095]
11. Holgado BL, Guerreiro Stucklin A, Garzia L, Daniels C & Taylor MD Tailoring Medulloblastoma Treatment Through Genomics: Making a Change, One Subgroup at a Time. Annu Rev Genomics Hum Genet 18, 143–166 (2017). [PubMed: 28475368]
12. Volpe JJ Cerebellum of the premature infant: rapidly developing, vulnerable, clinically important. J Child Neurol 24, 1085–1104 (2009). [PubMed: 19745085]
13. Johnson MB, et al. Functional and evolutionary insights into human brain development through global transcriptome analysis. Neuron 62, 494–509 (2009). [PubMed: 19477152]
14. Kang HJ, et al. Spatio-temporal transcriptome of the human brain. Nature 478, 483–489 (2011). [PubMed: 22031440]
15. Li M, et al. Integrative functional genomic analysis of human brain development and neuropsychiatric risks. Science **362** (2018).**362**
16. Miller JA, et al. Transcriptional landscape of the prenatal human brain. Nature 508, 199–206 (2014). [PubMed: 24695229]
17. Mu Q, Chen Y & Wang J Deciphering Brain Complexity Using Single-cell Sequencing. Genomics Proteomics Bioinformatics 17, 344–366 (2019). [PubMed: 31586689]
18. Rosenberg AB, et al. Single-cell profiling of the developing mouse brain and spinal cord with split-pool barcoding. Science 360, 176–182 (2018). [PubMed: 29545511]
19. Zhang B & Horvath S A general framework for weighted gene co-expression network analysis. Stat Appl Genet Mol Biol 4, Article17 (2005).
20. Lange W Cell number and cell density in the cerebellar cortex of man and some other mammals. Cell Tissue Res 157, 115–124 (1975). [PubMed: 804353]
21. McGinnis CS, Murrow LM & Gartner ZJ DoubletFinder: Doublet Detection in Single-Cell RNA Sequencing Data Using Artificial Nearest Neighbors. Cell Syst 8, 329–337 e324 (2019). [PubMed: 30954475]
22. Aldinger KA, et al. Redefining the Etiologic Landscape of Cerebellar Malformations. Am J Hum Genet 105, 606–615 (2019). [PubMed: 31474318]

23. Butler A, Hoffman P, Smibert P, Papalexi E & Satija R Integrating single-cell transcriptomic data across different conditions, technologies, and species. Nat Biotechnol 36, 411–420 (2018). [PubMed: 29608179]
24. Machold R & Fishell G Math1 is expressed in temporally discrete pools of cerebellar rhombic-lip neural progenitors. Neuron 48, 17–24 (2005). [PubMed: 16202705]
25. Wang VY, Rose MF & Zoghbi HY Math1 expression redefines the rhombic lip derivatives and reveals novel lineages within the brainstem and cerebellum. Neuron 48, 31–43 (2005). [PubMed: 16202707]
26. Englund C, et al. Unipolar brush cells of the cerebellum are produced in the rhombic lip and migrate through developing white matter. J Neurosci 26, 9184–9195 (2006). [PubMed: 16957075]
27. Cao J, et al. The single-cell transcriptional landscape of mammalian organogenesis. Nature 566, 496–502 (2019). [PubMed: 30787437]
28. Fink AJ, et al. Development of the deep cerebellar nuclei: transcription factors and cell migration from the rhombic lip. J Neurosci 26, 3066–3076 (2006). [PubMed: 16540585]
29. Zecevic N & Rakic P Differentiation of Purkinje cells and their relationship to other components of developing cerebellar cortex in man. J Comp Neurol 167, 27–47 (1976). [PubMed: 818132]
30. Dastjerdi FV, Consalez GG & Hawkes R Pattern formation during development of the embryonic cerebellum. Front Neuroanat 6, 10 (2012). [PubMed: 22493569]
31. Emmert-Buck MR, et al. Laser capture microdissection. Science 274, 998–1001 (1996). [PubMed: 8875945]
32. Espina V, et al. Laser-capture microdissection. Nat Protoc 1, 586–603 (2006). [PubMed: 17406286]
33. Newman AM, et al. Determining cell type abundance and expression from bulk tissues with digital cytometry. Nat Biotechnol 37, 773–782 (2019). [PubMed: 31061481]
34. Liu J, et al. Jointly defining cell types from multiple single-cell datasets using LIGER. Nat Protoc 15, 3632–3662 (2020). [PubMed: 33046898]
35. Welch JD, et al. Single-Cell Multi-omic Integration Compares and Contrasts Features of Brain Cell Identity. Cell 177, 1873–1887 e1817 (2019). [PubMed: 31178122]
36. Vladoiu MC, et al. Childhood cerebellar tumours mirror conserved fetal transcriptional programs. Nature 572, 67–73 (2019). [PubMed: 31043743]
37. Van De Weghe JC, et al. Mutations in ARMC9, which Encodes a Basal Body Protein, Cause Joubert Syndrome in Humans and Ciliopathy Phenotypes in Zebrafish. Am J Hum Genet 101, 23–36 (2017). [PubMed: 28625504]
38. Feliciano P, et al. Exome sequencing of 457 autism families recruited online provides evidence for autism risk genes. NPJ Genom Med 4, 19 (2019). [PubMed: 31452935]
39. RK CY, et al. Whole genome sequencing resource identifies 18 new candidate genes for autism spectrum disorder. Nat Neurosci 20, 602–611 (2017). [PubMed: 28263302]
40. Ruzzo EK, et al. Inherited and De Novo Genetic Risk for Autism Impacts Shared Networks. Cell 178, 850–866 e826 (2019). [PubMed: 31398340]
41. Willsey AJ, et al. The Psychiatric Cell Map Initiative: A Convergent Systems Biological Approach to Illuminating Key Molecular Pathways in Neuropsychiatric Disorders. Cell 174, 505–520 (2018). [PubMed: 30053424]
42. Yuen RK, et al. Whole-genome sequencing of quartet families with autism spectrum disorder. Nat Med 21, 185–191 (2015). [PubMed: 25621899]
43. De Strooper B & Karran E The Cellular Phase of Alzheimer's Disease. Cell 164, 603–615 (2016). [PubMed: 26871627]
44. Bis JC, et al. Whole exome sequencing study identifies novel rare and common Alzheimer's-Associated variants involved in immune response and transcriptional regulation. Mol Psychiatry (2018).
45. Wizeman JW, Guo Q, Wilion EM & Li JY Specification of diverse cell types during early neurogenesis of the mouse cerebellum. Elife 8 (2019).
46. Hovestadt V, et al. Resolving medulloblastoma cellular architecture by single-cell genomics. Nature 572, 74–79 (2019). [PubMed: 31341285]

47. Carter RA, et al. A Single-Cell Transcriptional Atlas of the Developing Murine Cerebellum. Curr Biol 28, 2910–2920 e2912 (2018). [PubMed: 30220501]
48. Sillitoe RV & Joyner AL Morphology, molecular codes, and circuitry produce the three-dimensional complexity of the cerebellum. Annu Rev Cell Dev Biol 23, 549–577 (2007). [PubMed: 17506688]
49. Nakatani T, Minaki Y, Kumai M, Nitta C & Ono Y The c-Ski family member and transcriptional regulator Corl2/Skor2 promotes early differentiation of cerebellar Purkinje cells. Dev Biol 388, 68–80 (2014). [PubMed: 24491816]
50. Haldipur P, et al. Preterm delivery disrupts the developmental program of the cerebellum. PLoS One 6, e23449 (2011). [PubMed: 21858122]
51. Gerrelli D, Lisgo S, Copp AJ & Lindsay S Enabling research with human embryonic and fetal tissue resources. Development 142, 3073–3076 (2015). [PubMed: 26395135]
52. Dobin A, et al. STAR: ultrafast universal RNA-seq aligner. Bioinformatics 29, 15–21 (2013). [PubMed: 23104886]
53. Anders S, Pyl PT & Huber W HTSeq--a Python framework to work with high-throughput sequencing data. Bioinformatics 31, 166–169 (2015). [PubMed: 25260700]
54. Love MI, Huber W & Anders S Moderated estimation of fold change and dispersion for RNA-seq data with DESeq2. Genome Biol 15, 550 (2014). [PubMed: 25516281]
55. Szklarczyk D, et al. STRING v11: protein-protein association networks with increased coverage, supporting functional discovery in genome-wide experimental datasets. Nucleic Acids Res 47, D607–D613 (2019). [PubMed: 30476243]
56. DeLuca DS, et al. RNA-SeQC: RNA-seq metrics for quality control and process optimization. Bioinformatics 28, 1530–1532 (2012). [PubMed: 22539670]
57. Hodge RD, et al. Conserved cell types with divergent features in human versus mouse cortex. Nature 573, 61–68 (2019). [PubMed: 31435019]
58. Stuart T, et al. Comprehensive Integration of Single-Cell Data. Cell 177, 1888–1902 e1821 (2019). [PubMed: 31178118]
59. Mirzaa GM, et al. De novo and inherited variants in ZNF292 underlie a neurodevelopmental disorder with features of autism spectrum disorder. Genet Med 22, 538–546 (2020). [PubMed: 31723249]
60. Epting D, et al. Loss of CBY1 results in a ciliopathy characterized by features of Joubert syndrome. Hum Mutat 41, 2179–2194 (2020). [PubMed: 33131181]
61. Latour BL, et al. Dysfunction of the ciliary ARMC9/TOGARAM1 protein module causes Joubert syndrome. J Clin Invest 130, 4423–4439 (2020). [PubMed: 32453716]
62. Luo M, et al. Disrupted intraflagellar transport due to IFT74 variants causes Joubert syndrome. Genet Med (2021).
63. Sanders SJ, et al. Insights into Autism Spectrum Disorder Genomic Architecture and Biology from 71 Risk Loci. Neuron 87, 1215–1233 (2015). [PubMed: 26402605]
64. Deciphering Developmental Disorders S Prevalence and architecture of de novo mutations in developmental disorders. Nature 542, 433–438 (2017). [PubMed: 28135719]
65. Rauch A, et al. Range of genetic mutations associated with severe non-syndromic sporadic intellectual disability: an exome sequencing study. Lancet 380, 1674–1682 (2012). [PubMed: 23020937]
66. Irizarry RA, Wang C, Zhou Y & Speed TP Gene set enrichment analysis made simple. Stat Methods Med Res 18, 565–575 (2009). [PubMed: 20048385]